Thermal Science and Engineering Progress 36 (2022) 101525

Contents lists available at ScienceDirect

Thermal Science and Engineering Progress

journal homepage: www.sciencedirect.com/journal/thermal-science-and-engineering-progress

Energetic and exergetic study of a potential interconnection of a natural gas engine, heat pumps with a thermal and a mechanical compressor

Gábor L. Szabó

University of Debrecen, Faculty of Engineering, Department of Building Services and Building Engineering, 4028 Debrecen, Ótemető Str. 2-4, Hungary

ARTICLE INFO

Keywords:
Heat pump
Absorption chiller
Gas engine
Exergy
CCHP system

ABSTRACT

HVAC systems in buildings are significant energy consumers. It is proposed to utilize energy production systems that allow the generation of several types of energy from the same primary energy source. A solution of a CCHP, which consists of two types of heat pumps and a gas engine, was analysed in this article. The analysed solution can work in three operating modes, which allows the operators to avoid running both heat pumps, e.g., in the case of reduced demand or maintenance problems. These three operating modes are compared from energetical and exergetical. For a qualitative comparison of the operating modes, PXR is defined, and COP of heat pumps with a mechanical compressor is specified in an alternative way. Simplified equations are developed to determine PER and PXR to facilitate comparison. These equations can also be used to calculate the cases where the energy produced by the gas engine is not necessarily fully utilized by the heat pumps.

The comparisons are also made via a case study. It is concluded that operating both heat pumps is the best option from energetical, but from exergetical, it is the worst. From the exergetical, if the required chilled water temperature is higher than 15.67 °C, or if the external air temperature is lower than 32.22 °C, then it is advisable to operate only the absorption heat pump from the gas engine. From the energetical, this can only be the second-best option if the generator temperature is above 85.02 °C.

Introduction

As urbanization quickens, the energy consumption of heating, ventilation, and air conditioning (HVAC) is increasing in buildings. Above 40 % of energy consumption in the European Union [1] and up to 60 % globally [2] is related to buildings. Therefore, saving energy is one of the main tasks of the construction industry [3]. The cooling and heating energy demands of buildings are affected by several factors [4], but they can be reduced, for example, by using thermal insulation [5,6] or the use of carefully planned natural ventilation [7]. The heat losses in HVAC systems can also be reduced, for example, by recycling heat losses (in the energy flow of buildings) [8] or insulating components [9].

The required heat, cold, and electric power can be generated from different energy sources by energy producers in HVAC systems. The energy production technologies that can produce all three concurrently are known as combined cooling, heat, and power (CCHP) systems. [10] These systems are the multiple productions of energy from the same primary energy source. [11] These technologies could be an appropriate way to increase thermal efficiency, reduce energy consumption and operating costs, and produce cleaner energy. [12].

Of course, CCHP systems have been the subject of many studies. Sheykhi et al. [10] showed a payback of almost four years for a CCHP system with a Stirling engine and absorption chiller. Balakheli et al. [13] investigated five different CCHP system configurations from an energetic and economic points of view. They concluded that the best option would be the chiller with the mechanical compressor driven by an internal combustion engine, and the waste heat from the engine recovered. The question may arise as to whether it would not be preferable to replace fossil fuels with renewable energy, at least in part. Wang et al. [14] evaluated the integrability of solar energy and determined that while it would be a superior option in some circumstances, waste heat recovery is even better under present conditions. Wu and Wang [15] reviewed numerous research and concluded that the main engines of CCHP systems continue to use fossil fuels in the foreseeable future because the renewable energy systems cannot fully and economically replace them.

Several indicators can be used to evaluate CCHP systems, but previous studies have not shown how these can be utilized rationally to exploit their specific advantages. Ma et al. [16] investigated the underlying effects of three general energy indicators (the primary energy ratio, primary energy saving ratio, and annual average comprehensive

E-mail address: l.szabo.gabor@eng.unideb.hu.

https://doi.org/10.1016/j.tsep.2022.101525
Received 15 July 2022; Received in revised form 20 October 2022; Accepted 20 October 2022
Available online 26 October 2022

Nomenclature

COP_{AC}	is the coefficient of performance (cooling mode, absorption heat pump), in [-].
COP_{RC}	is the coefficient of performance (cooling mode, heat pump with mechanical compressor), in [-].
Ex_{elect}	is the exergy content of "P_{elect}", in W.
Ex_{fuel}	is the exergy content of "Q_{fuel}", in W.
Ex_P	is the exergy content of "P", in W.
LHV	is the lower heating value of fuel, in J/m^3.
P	is the electric power consumed by a heat pump with mechanical compressor, in W.
P_{elctr}	is the electric power delivered by the gas engine, in W.
PER	is the primary energy ratio, in [-].
PXR	is the primary exergy ratio, in [-].
$\dot{Q}_{0,1}$	is the cooling capacity (heat pump with mechanical compressor), in W.
$\dot{Q}_{0,2}$	is the cooling capacity (absorption heat pump), in W.
$\dot{Q}_{fuel}$	is the chemical energy flow produced from natural gas, in W.
$\dot{Q}_G$	is the heat consumed in the generator, in W.
$\dot{Q}_{H,1}$	is the heat released in the condenser (heat pump with mechanical compressor), in W.
$\dot{Q}_{term}$	is the thermal energy flow delivered by the gas engine, in W.
S_R	is the generated entropy within the refrigerant cycle, in W/K.
T_A	is the temperature in the absorber, in K.
$T_{c,1}$; $T_{c,2}$	is the supply and return temperature of chilled water, in K.
T_e	is the air temperature around the machines, in K.
T_G	is the temperature in the generator, in K.
$T_{g,1}$; $T_{g,2}$	is the temperature of warm water entering and leaving the generator, in K.
$T_{h,1}$; $T_{h,2}$	is the supply and return temperature of heating fluid (heat pump with mechanical compressor), in K.
$T_{h,3}$; $T_{h,4}$	is the supply and return temperature of heating fluid (absorption heat pump), in K.
$T_{H,A}$	is the condensing temperature (absorption heat pump), in K.
$T_{H,R}$	is the condensing temperature (heat pump with mechanical compressor), in K.
$T_{L,A}$	is the evaporating temperature (absorption heat pump), in K.
$T_{L,R}$	is the evaporating temperature (heat pump with mechanical compressor), in K.
T_X	is the reference temperature, in K.
V_{fuel}	is the volume flow of the natural gas, in m^3/s.
α_{elect}	is the consumption share of the electric power, in [-].
α_{term}	is the consumption share of the thermal energy flow, in [-].
β	is the thermo-chemical performance index, in [-].
δ_R	is the coefficient of compensation for entropy-surplus, in 1/K.
ΔEX_G	is the exergy content of the thermal energy flow delivered to the generator, in W.
$\Delta Ex_{sec,C1}$	is the exergy content of the cold energy flow delivered by the heat pump with mechanical compressor, in W.
$\Delta Ex_{sec,C2}$	is the exergy content of the cold energy flow delivered by the absorption heat pump, in W.
$\Delta Ex_{sec,H1}$	is the exergy content of the heat energy flow delivered by the heat pump with mechanical compressor, in W.
$\Delta Ex_{sec,H2}$	is the exergy content of the heat energy flow delivered by the absorption heat pump, in W.
ΔEx_{term}	is the exergy content of the thermal energy flow delivered by the gas engine, in W.
ΔT_C	is the different between the supply and return temperature of chilled water, in K.
ΔT_H	is the different between the supply and return temperature of heating fluid, in K.
φ_{NG}	is the exergy calculation factor for natural gas, in [-].
η_{elect}	is the electric efficiency of a gas engine in %.
$\eta_{sys,AC}$	is the total exergy system efficiency (cooling mode, absorption heat pump), in %.
$\eta_{sys,AH}$	is the total exergy system efficiency (heating mode, absorption heat pump), in %.
$\eta_{sys,RC}$	is the total exergy system efficiency (cooling mode, heat pump with mechanical compressor), in %.
$\eta_{sys,RH}$	is the total exergy system efficiency (heating mode, heat pump with mechanical compressor), in %.
η_{term}	is the thermal efficiency of a gas engine, in %.

energy utilization efficiency). Based on their results, when the system configuration and operating strategy are the same, the primary energy ratio and primary energy savings ratio indicators have the same optimizing effect. Furthermore, the difference between the primary energy ratio ("PER") values of the CCHP and the reference system can show whether carbon emissions are decreasing.

One type of CCHP system is the gas engine heat pump (GEHP). The GEHP systems are in high demand due to their efficiency, environmental benefits, and energy-saving potential [17]. The recovery of waste heat is one of the main issues for GEHP systems. It is mainly used to generate domestic hot water, where the PER value can reach 1.83 as well. [18]. Another solution (the GECAHP system) is to use waste heat to drive an absorption chiller (chiller with a thermal compressor). Its prototype was created by Sun and Guo [19] and achieved a "PER" value of 1.81. According to their experiments, compared to traditional GEHP systems, up to a quarter of primary energy can be saved. Liu et al. analysed a GECAHP system where the two heat pumps are parallel-connected. [20]. It has been shown that compared to a conventional GEHP system, it is possible to achieve 6 % higher heating performance and a 5 % primary energy savings, while achieving a "PER" value above 1.5. Liu et al. proposed a GECAHP system that connects the two heat pumps in series to increase the heating capacity at low air temperatures [21]. They conclude that compared to a conventional GEHP system, the heating capacity increases, but the primary energy ratio is only between 1.0 and 1.1.

GEHP and GEACHP systems are commonly used for cogeneration or only heating or cooling rather than trigeneration. In such cases, the systems can be optimized for either cooling only or heating. Sun [22] examined a GEHP system designed just for cooling, and the chiller water was produced by an absorption chiller and a vapour-compression chiller. The "PER" value of the system was 1.84. The system did not utilize the generated heat by the chillers, and the electricity generated was fully used by the vapour-compression chiller. Liu et al. [23] developed a GEHP system designed just for cooling, using an evaporative condenser. The system achieved a maximum "PER" value of 1.55. Zhang et al. [24] investigated the heating and cooling applicability of gas engine heat pumps in different building types in winter and summer. The efficiency was increased by energy storage. The value of "PER" was 1.448/1.167 (winter/summer) for office; 1.427/1.158 (winter/summer) for university and 1.392/1.040 (winter/summer) for hotel.

As can be seen, there are several articles on trigeneration, but only a few examine GECAHP systems from an exergetic point of view. Furthermore, the impact on the value of the "PER", if the heat pumps might not fully utilize the energy generated by the gas engine, has not

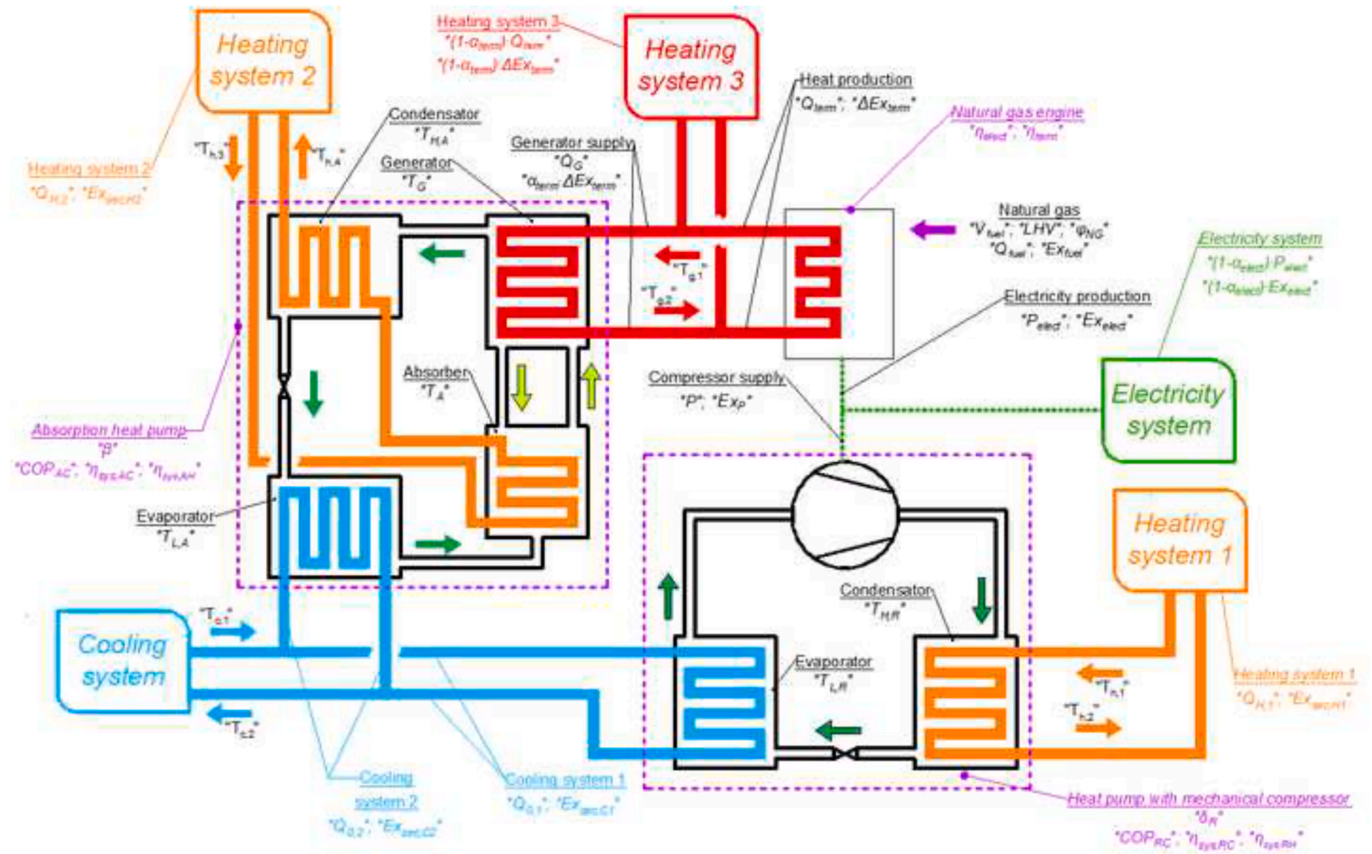

Fig. 1. The schema of the analysed system.

Table 1
The examined trigeneration operation modes.

No.	Operated machines	Generated energies
1	Gas engine Heat pump with a mechanical compressor	Electrical power (if $\alpha_{elect} < 1$) Cooling capacity Heating energy flow with a high exergy content Heating energy flow with a low exergy content
2	Gas engine Absorption heat pump	Electrical power Cooling capacityHeating energy flow with a high exergy content (if $\alpha_{term} < 1$) Heating energy flow with a low exergy content
3	Gas engine Heat pump with a mechanical compressor Absorption heat pump	Electrical power (if $\alpha_{elect} < 1$) Cooling energyHeating energy flow with a high exergy content (if $\alpha_{term} < 1$) Heating energy flow with a low exergy content

Table 2
Parameters of the sensitivity analysing.

Analysed factor	The reference value	The range of values
COP_{RC}	*2.73*	*0–5.3*
COP_{AC}	*0.69*	*0–1.28*
η_{elect}	*35.7 %*	*0 %-50.9 %*
η_{term}	*49.1 %*	*0 %-64.3 %*
α_{elect}	*0.28*	*0–1*
α_{term}	*0.49*	*0–1*

been examined. What happens when, for example, both types of heat pumps are not running due to maintenance problems or cost savings is also not investigated.

The system to be investigated, the possible trigeneration modes, and the research's theoretical background are described below. Based on this, an energetic and exergetic comparison with the trigeneration operating modes is conducted. Where necessary, new or simplified equations are defined. Sensitivity analysis is applied to reveal the appropriate intervention points. As such equations provide difficult-to-measure quantities, easier-to-measure temperature values are also given to the developed equations. Finally, a case study was employed to assess the correctness and applicability of the equations.

Materials and methods

There are several design alternatives for GECAHP systems. In the following, the configuration options in Fig. 1 are examined.

The chemical energy input (Equation (1)) to the gas engine and its exergy content (Equation (2)) [25]:

$$\dot{Q}_{fuel} = LHV \bullet \dot{V}_{fuel}, [W] \tag{1}$$

$$Ex_{fuel} = \varphi_{NG} \bullet LHV \bullet \dot{V}_{fuel}, [W] \tag{2}$$

Where „LHV" is the lower heating value of fuel, in J/m^3, „V_{fuel}" is the volume flow of the natural gas, in m^3/s, „φ_{NG}" is the exergy calculation factor for natural gas, based on [25] is 1.04 ± 0.5 %.

The gas engine burns natural gas to produce electric power (Equation (3)) and heat (Equation (4)). The quantity of these:

$$P_{elect} = \frac{\eta_{elect}}{100} \bullet \dot{Q}_{fuel}; [W] \tag{3}$$

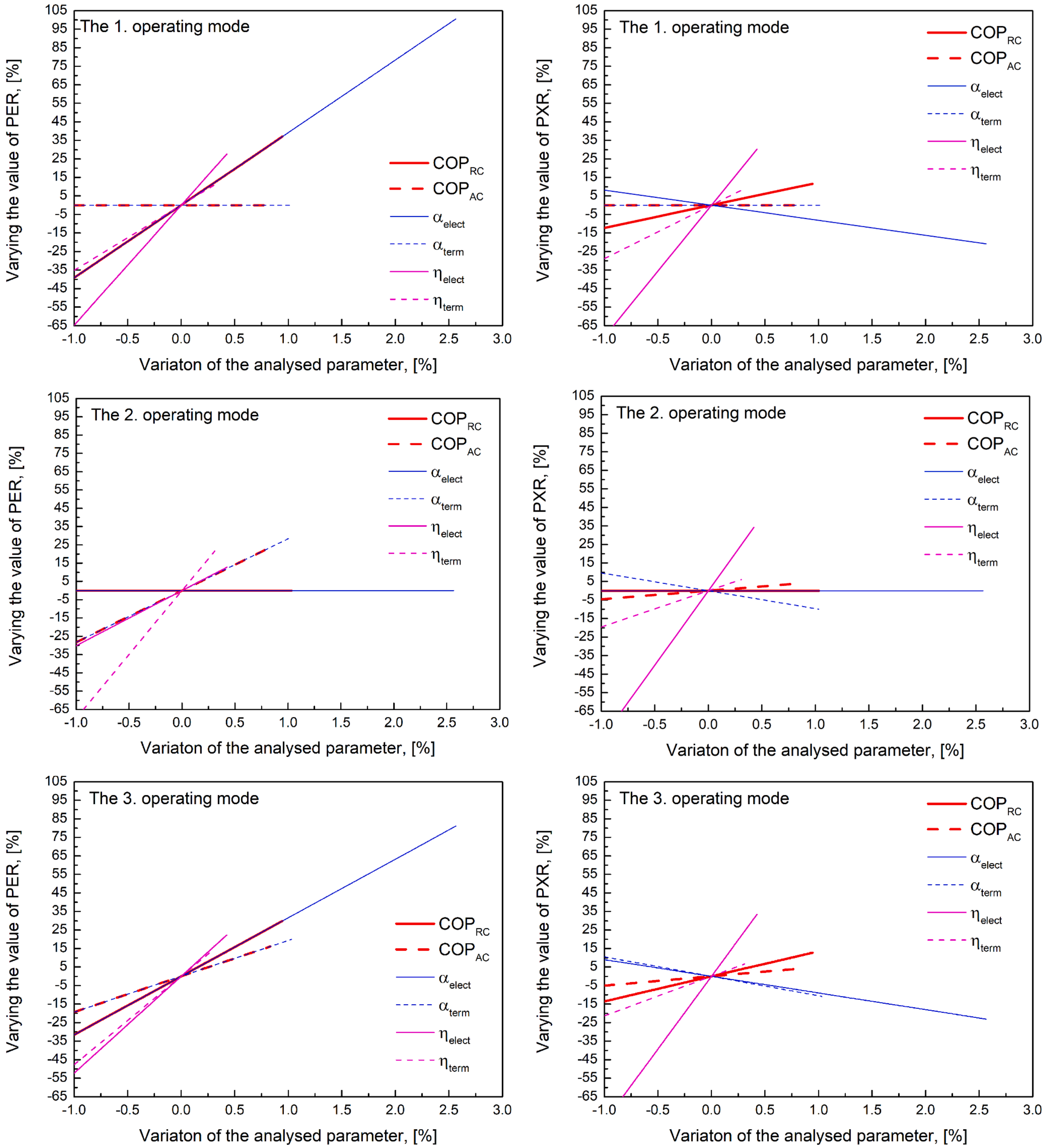

Fig. 2. Sensitivity of PER and PXR depending on the coefficient of perfomance, the consumption shares and the efficiencies of a gas engine (**a**) the 1. operating mode, PER; (**b**) the 1. operating mode, PXR; (**c**) the 2. operating mode, PER; (**d**) the 2. operating mode, PXR; (**e**) the 3. operating mode, PER; (**f**) the 3. operating mode, PXR;

$$\dot{Q}_{term} = \frac{\eta_{term}}{100} \bullet \dot{Q}_{fuel}; [W] \tag{4}$$

Where „η_{elect}" is the electric efficiency of, and „η_{term}" is the thermal efficiency of a gas engine, in %.

Exergy contents of the energies produced [26,27]:

$$Ex_{elect} \cong P_{elect}; [W] \tag{5}$$

$$\Delta Ex_{term} = \frac{\eta_{term}}{100} \bullet \dot{Q}_{fuel} \bullet \left[1 - \frac{T_e \bullet T_X}{T_{g,1} \bullet T_{g,2}}\right]; [W] \tag{6}$$

Where „T_e" is the air temperature around the machines, in K, „T_X" is the reference temperature, in K, and „$T_{g,1}$" és a „$T_{g,2}$" is the temperature of warm water entering and leaving the gas engine, in K.

Generated energies by a gas engine can be utilized to a different extent by the heat pumps. The consumption share is the ratio between the extent of energy consumed by heat pumps and the amount of the same kind of energy produced by the gas engine. Applying this to electrical power (Equation (7)) and thermal energy flow (Equation (8)):

$$\alpha_{elect} = \frac{P}{P_{elect}} = \frac{Ex_P}{Ex_{elect}}, [-] \tag{7}$$

$$\alpha_{term} = \frac{\dot{Q}_G}{\dot{Q}_{term}} = \frac{\Delta Ex_G}{\Delta Ex_{term}}, [-] \tag{8}$$

Where “P” is the electric power consumed by a heat pump with a mechanical compressor, in W; “ΔEX_P” is the exergy content of “P”, in W. “$\dot{Q}_G$” is the heat consumed in the absorption heat pump (its generator), in W, “ΔEX_G is the exergy content of the thermal energy flow delivered to the generator, in W.

The amount of energy flows produced by heat pumps can be given using the coefficient of performance of cooling (“COP_C”), as well. [27,28]. The value of “COP_C” is given by Equation (9) for a heat pump with a mechanical compressor and by Equation (10) for a heat pump with a thermal compressor:

$$COP_{RC} = \frac{\dot{Q}_{0,1}}{P} = \frac{\dot{Q}_{0,1}}{\alpha_{elect} \bullet P_{elect}}, [-] \tag{9}$$

$$COP_{AC} = \frac{\dot{Q}_{0,2}}{\dot{Q}_G} = \frac{\dot{Q}_{0,2}}{\alpha_{term} \bullet \dot{Q}_{term}} = \frac{T_{L,A}}{T_A} \bullet \frac{T_{H,A} - T_A}{T_{H,A} - T_{L,A}} \bullet \beta + \frac{T_{L,A}}{T_G} \bullet \frac{T_G - T_{H,A}}{T_{H,A} - T_{L,A}}, [-] \tag{10}$$

Where “$\dot{Q}_{0,1}$” and “$\dot{Q}_{0,2}$” are the cooling capacities of the heat pump with a mechanical compressor and absorption heat pump. “$T_{L,A}$” is the evaporating temperature of the absorption heat pump, in K; “$T_{H,A}$” is the condensing temperature of the absorption heat pump, in K; “T_A” is the temperature in the absorber, in K; “T_G” is the temperature in the generator, in K. “β” is the thermo-chemical performance index.

The exergy content of energy flows produced by heat pumps can be provided using the total exergetic system efficiency (“η_{sys}”), as well [26,27,29]. Equation (11) gives the exergy content of the generated cold energy flow by the heat pump with a mechanical compressor, while Equation (12) gives the exergy content of the generated heat energy flow. For the heat pump with a thermal compressor, Equation (13) can give the exergy content of the produced cold energy flow, and Equation (14) can provide the exergy content of the generated heat energy flow.

$$\begin{aligned}\eta_{sys,RC} &= \frac{\Delta Ex_{sec,C1}}{Ex_P} \bullet 100 = \frac{\Delta Ex_{sec,C1}}{\alpha_{elect} \bullet P_{elect}} \bullet 100 \\ &= COP_{RC} \bullet \left[\frac{T_e \bullet T_X}{T_{c,1} \bullet T_{c,2}} - 1\right] \bullet 100, [\%]\end{aligned} \tag{11}$$

$$\begin{aligned}\eta_{sys,RH} &= \frac{\Delta Ex_{sec,H1}}{Ex_P} \bullet 100 = \frac{\Delta Ex_{sec,H1}}{\alpha_{elect} \bullet P_{elect}} \bullet 100 \\ &= [COP_{RC} + 1] \bullet \left[1 - \frac{T_e \bullet T_X}{T_{h,1} \bullet T_{h,2}}\right] \bullet 100, [\%]\end{aligned} \tag{12}$$

$$\begin{aligned}\eta_{sys,AC} &= \frac{\Delta Ex_{sec,C2}}{\Delta Ex_G} \bullet 100 = \frac{\Delta Ex_{sec,C2}}{\alpha_{term} \bullet \Delta Ex_{term}} \bullet 100 \\ &= COP_{AC} \bullet \left[\frac{T_e \bullet T_X}{T_{c,1} \bullet T_{c,2}} - 1\right] \bullet \frac{T_{g,1} \bullet T_{g,2}}{T_{g,1} \bullet T_{g,2} - T_e \bullet T_X} \bullet 100, [\%]\end{aligned} \tag{13}$$

$$\begin{aligned}\eta_{sys,AH} &= \frac{\Delta Ex_{sec,H2}}{\Delta Ex_G} \bullet 100 = \frac{\Delta Ex_{sec,H2}}{\alpha_{term} \bullet \Delta Ex_{term}} \bullet 100 \\ &= [COP_{AC} + 1] \bullet \left[1 - \frac{T_e \bullet T_X}{T_{h,3} \bullet T_{h,4}}\right] \bullet \frac{T_{g,1} \bullet T_{g,2}}{T_{g,1} \bullet T_{g,2} - T_e \bullet T_X} \bullet 100, [\%]\end{aligned} \tag{14}$$

Where “$\Delta Ex_{sec,C1}$” and “$\Delta Ex_{sec,H1}$” are the exergy contents of the cold and heat energy flow delivered by a heat pump with a mechanical compressor, in W. “$\Delta Ex_{sec,C2}$” and “$\Delta Ex_{sec,H2}$” are the exergy contents of the cold and heat energy flow delivered by an absorption heat pump, in W. Furthermore, “$T_{h,1}$” and “$T_{h,2}$” is the supply and return temperature of heating fluid by a heat pump with a mechanical compressor, “$T_{h,3}$” and “$T_{h,4}$” is the supply and return temperature of heating fluid by absorption heat pump, in K. Finally, “$T_{c,1}$” and “$T_{c,2}$” is the supply and return temperature of chilled water, in K.

The primary energy ratio (which is a similar indicator to the “COP_C”) can be employed to describe the energy efficiency of a complex system (e.g. [20,30]):

$$PER = \frac{the\ useful\ energy\ flow}{the\ input\ energy\ flow}, [-] \tag{15}$$

Results

The coefficient of compensation for entropy-surplus

The value of “COP_C” by an absorption heat pump (heat pump with a thermal compressor) can also be given using the main operating temperatures and an index (“β”). If this is to be done for a heat pump with a mechanical compressor, it is necessary to define the energy flow (Equation (16)) and entropy balance equation (Equation (17)) for these machines [31]:

$$\dot{Q}_{0,1} + P = \dot{Q}_{H,1}, [W] \tag{16}$$

$$\frac{\dot{Q}_{0,1}}{T_{L,R}} + S_r = \frac{\dot{Q}_{H,1}}{T_{H,R}}, [-] \tag{17}$$

Where „$\dot{Q}_{H,1}$″ is the heat released in the condenser by heat pump with mechanical compressor, in W. “$T_{L,R}$” is the evaporating temperature by heat pump with mechanical compressor, in K; and “$T_{H,R}$” is the condensing temperature by heat pump with mechanical compressor, in K. “S_r” is the generated entropy within the refrigerant cycle, in W/K.

The “δ_R” as the coefficient of compensation for entropy-surplus is introduced:

$$0 \le \delta_R = \frac{S_r}{P} \le \frac{1}{T_{H,R}}, \left[\frac{1}{K}\right] \tag{18}$$

The value of “COP_{RC}” can also be calculated using the operating temperatures and “δ_R” by utilizing equations (9) and (15)–(17).

$$COP_{RC} = \frac{T_{L,R}}{T_{H,R} - T_{L,R}} \bullet \left(1 - T_{H,R} \bullet \delta_R\right), [-] \tag{19}$$

At both extreme values of “δ_R”, “COP_{RC}” also takes its extreme values. The value of “COP_{RC}” increases as the value of “δ_R” decreases. If the heat pump could not absorb enough external electrical power to compensate for the generated entropy within the refrigerant cycle, the value of “δ_R” would be higher than “$1/T_{H,R}$.

The primary exergy ratio

An indicator similar to “η_{sys}” is required to describe exergy efficiency for complex systems. By analogy with “PER”, the primary exergy ratio (“PXR”) is introduced:

$$PXR = \frac{the\ nergy\ content\ of\ useful\ energy\ flow}{the\ energy\ content\ of\ input\ energy\ flow}, [-] \tag{20}$$

Simplified “PER” and “PXR” equations for the examined GECAHP system

From the GECAHP system shown in Fig. 1, three operating modes can be formed, with each of which electrical power, cooling capacity, and heat energy flow can also be simultaneously extracted from the system. These modes are shown in Table 1:

For each of the three operating modes, the value of “PER” can be given using Equations (3), (4), (7), (8), (9), (10), and (15). Equations (21)-(23) respectively give the “PER” values for the 1., 2., and 3.

operating modes.

$$PER_1 = \frac{\eta_{term}}{100} + \frac{\eta_{elect}}{100} + 2 \bullet \frac{\eta_{elect}}{100} \bullet \alpha_{elect} \bullet COP_{RC}, [-] \tag{21}$$

$$PER_2 = 2 \bullet \alpha_{term} \bullet \frac{\eta_{term}}{100} \bullet COP_{AC} + \frac{\eta_{term}}{100} + \frac{\eta_{elect}}{100}, [-] \tag{22}$$

$$PER_3 = \frac{\eta_{elect}}{100} + \frac{\eta_{term}}{100} + 2 \bullet \frac{\eta_{elect}}{100} \bullet \alpha_{elect} \bullet COP_{RC} + 2 \bullet \frac{\eta_{term}}{100} \bullet \alpha_{term} \bullet COP_{AC}, [-] \tag{23}$$

The value of „PXR" in the three operating modes can be determined using equations (5)–(8), (11)–(14), and (20). Equations (24)-(26) respectively can give the "PXR" values for the 1., 2., and 3. operating modes.

$$PXR_1 = \frac{\eta_{term}}{100 \bullet \varphi_{NG}} \bullet \left[1 - \frac{T_e \bullet T_X}{T_{g,1} \bullet T_{g,2}}\right] + \frac{\eta_{elect}}{100 \bullet \varphi_{NG}} \bullet \left[1 - \alpha_{elect} \bullet \left(1 - \frac{\eta_{sys,RC}}{100} - \frac{\eta_{sys,RH}}{100}\right)\right], [-] \tag{24}$$

$$PXR_2 = \frac{\eta_{elect}}{100 \bullet \varphi_{NG}} + \frac{\eta_{term}}{100 \bullet \varphi_{NG}} \bullet \left(1 - \frac{T_e \bullet T_X}{T_{g,1} \bullet T_{g,2}}\right) \bullet \left[1 - \alpha_{term} \bullet \left(1 - \frac{\eta_{sys,AC}}{100} - \frac{\eta_{sys,AH}}{100}\right)\right], [-] \tag{25}$$

$$PXR_3 = \frac{\eta_{elect}}{100 \bullet \varphi_{NG}} \bullet \left[1 - \alpha_{elect} \bullet \left(1 - \frac{\eta_{sys,RC}}{100} - \frac{\eta_{sys,RH}}{100}\right)\right] + \frac{\eta_{term}}{100 \bullet \varphi_{NG}} \bullet \left(1 - \frac{T_e \bullet T_X}{T_{g,1} \bullet T_{g,2}}\right) \bullet \left[1 - \alpha_{term} \bullet \left(1 - \frac{\eta_{sys,AC}}{100} - \frac{\eta_{sys,AH}}{100}\right)\right], [-] \tag{26}$$

As can be observed, equations (21)-(26) are independent of the value of the fuels "LHV" and "V_{fuel}". The fuel quality is visible through "φ_{NG}", but only in equations (24)–(26).

Sensitivity analysis of "PER" and "PXR" value

The sensitivity of the "PER" and "PXR" values were examined for several factors. Table 2 summarises the range of values of these factors under study and their reference value. At values, the data of the machines in "4. Case Study" have also been taken into account.

Fig. 2. shown the results of the sensitivity analysis.

Based on Fig. 2, the values of "PER" and "PXR" have a higher sensitivity to changes in the gas engine efficiencies than to changes in the value of coefficients of performance or the consumption shares. There are linear relationships between the changes in the six analysed factors and the variation in the "PER" and "PXR" values, respectively. In degrees, the angles between the linear and the abscissa are given in Table 3.

Based on Table 2, for all three operating modes, the change in the value of η_{elect} primarily affects the values of "PXR", while "η_{term}" primarily affects the values of "PER". The consumption shares variation has the highest impact at the values for 3. operating mode. The changes in "COP" and "α" values have the same impact variation in "PER" values, while for variation in "PXR" values, the changes in "COP" values can achieve a higher impact.

Table 3
Angle of the "PER" and "PXR" variation.

	η_{elect}	η_{term}	α_{elect}	α_{term}	COP_{RC}	COP_{AC}
PER_1	*32.94*	*19.39*	*21.40*	*0.00*	*21.40*	*0.00*
PER2	*16.80*	*34.92*	*0.00*	*15.80*	*0.00*	*15.80*
PER_3	*27.59*	*25.52*	*17.54*	*10.96*	*17.54*	*10.96*
PXR_1	*35.43*	*16.09*	*4.66*	*0.00*	*6.99*	*0.00*
PXR_2	*38.80*	*11.09*	*0.00*	*5.51*	*0.00*	*2.64*
PXR_3	*38.18*	*12.06*	*5.15*	*6.00*	*7.72*	*2.88*

Table 4
The main data's of the machines.

Machine	Notation	Value
Chiller with mechanical compressor *(refrigerant: R134a)*	$\dot{Q}_{0,1}/P/\dot{Q}_{H1}$	595/218/813 kW
	Capacity control	59.5–595 kW
	$T_{L,R}/T_{H,R}$	3.75/55.96 °C
	$T_{c,2}/T_{c,1}$	8/14 °C
	$T_{h,1}/T_{h,2}$	35/46.2 °C
	δ_R	0.00147488
	$COP_{RC}/\eta_{sys,RC}/\eta_{sys,RH}$	2.73/32.64 %/30.73 %
Absorption chiller *(refrigerant-absorber: LiBr-H₂O)*	$\dot{Q}_{0,2}/\dot{Q}_G/\dot{Q}_{H2}$	910/1312.5/2154.6 kW
	Capacity control	364.2–1821 kW
	$T_{L,A}/T_{H,A}$	7.33/34 °C
	$T_{c,1}/T_{c,2}$	14/8 °C
	$T_{g,1}/T_{g,2}$	85/70 °C
	$T_{h,3}/T_{h,4}$	29.8/26 °C
	β	0.864
	$COP_{AC}/\eta_{sys,AC}/\eta_{sys,AH}$	0.693/31.33 %/1.64 %
Gas-engine *(natural gas)*	V_{fuel} (1 machine)	229 m^3/h
	η_{elect}/η_{term}	35.70 %/49.10 %
	Q_G/P_{elect} (1 machine)	531.1/388.3 kW
	φ_{NG}	1,04
Common data's	T_e	29 °C
	T_X	26 °C

Comparison of the three examined trigeneration operating modes from energetic and exergetic points of view

Equations (21)-(23) can be used to determine which mode of operation is the best choice from an energetic point of view.

$$PER_1 > PER_2; \ \ if \ \ COP_{RC} > \frac{\alpha_{term} \bullet \eta_{term}}{\alpha_{elect} \bullet \eta_{elect}} \bullet COP_{AC} \tag{27}$$

$$PER_3 > PER_1; \ \ if \ \ COP_{AC} > 0 \tag{28}$$

$$PER_3 > PER_2; \ \ if \ \ COP_{RC} > 0 \tag{29}$$

Based on equations (27)-(29), running both heat pumps will always be preferable from an energetic point of view. For industrial measurability, the equation (27) can be challenging, so this is presented for also a selected temperature. The chosen temperature is the generator temperature, which is one critical point for the efficient operation of absorption heat pumps.[32] Using equations (10), (19), and (27), the critical generator temperature where $PER_1 > PER_2$:

$$\frac{T_{H,A}}{1 + \frac{T_{H,A}-T_A}{T_A} \bullet \beta - \frac{\alpha_{elect} \bullet \eta_{elect}}{\alpha_{term} \bullet \eta_{term}} \bullet \frac{T_{H,A}-T_{L,A}}{T_{H,R}-T_{L,R}} \bullet \frac{T_{L,R}}{T_{L,A}} \bullet \left(1 - T_{H,R} \bullet \delta_R\right)} < T_G, [K] \tag{30}$$

Equations (24)-(26) can be utilized to investigate which mode of operation is the best choice from an exergetic point of view.

$PXR_1 > PXR_2$, if

$$\frac{\eta_{sys,RC}}{100} + \frac{\eta_{sys,RH}}{100} < 1 - \left[1 - \frac{T_{K,2} \bullet T_X}{T_{g,1} \bullet T_{g,2}}\right] \bullet \frac{\alpha_{term} \bullet \eta_{term}}{\alpha_{elect} \bullet \eta_{elect}} \bullet \left(1 - \frac{\eta_{sys,AC}}{100} - \frac{\eta_{sys,AH}}{100}\right) \tag{31}$$

$PXR_3 > PXR_1$, if

$$1 < \frac{\eta_{sys,AC}}{100} + \frac{\eta_{sys,AH}}{100} \tag{32}$$

$PXR_3 > PXR_2$, if

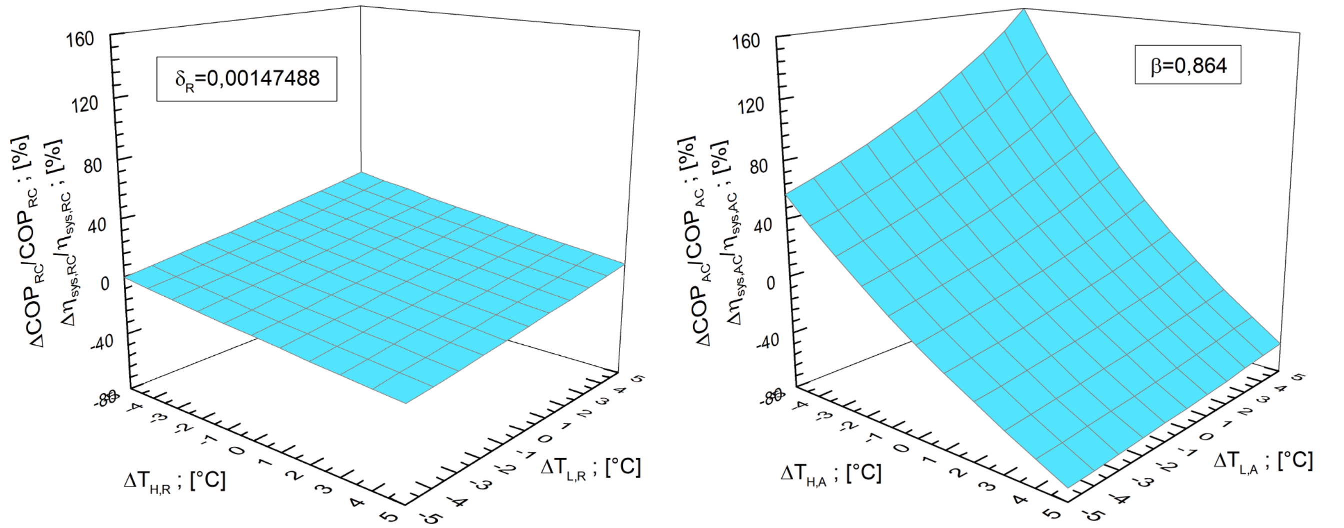

Fig. 3. Variation of values of "COP" and "η_{sys}" in cooling mode due to changes in the evaporating and condensing temperatures for **a)** the chiller with a mechanical compressor; **b)** the absorption chiller.

$$\frac{\eta_{sys,RC}}{100}+\frac{\eta_{sys,RH}}{100}>1 \tag{33}$$

The equations (31)–(34) are "translated" to two selected temperatures. The first is the supply temperature of chilled water if the $\Delta T_c = T_{c,2}$-$T_{c,1}$. The $PXR_1 > PXR_2$, if

$$T_{c,2}> -0,5\bullet\Delta T_c+\sqrt{\frac{\Delta T_c^{\,2}}{4}+\frac{T_e\bullet T_X\bullet COP_{RC}-T_e\bullet T_X\bullet\frac{\alpha_{term}\bullet\eta_{term}}{\alpha_{elect}\bullet\eta_{elect}}\bullet COP_{AC}}{\left(1-\frac{\eta_{sys,RH}}{100}\right)+COP_{RC}-\frac{\eta_{term}\bullet\alpha_{term}}{\alpha_{elect}\bullet\eta_{elect}}\bullet\left[\left(1-\frac{\eta_{sys,AH}}{100}\right)\bullet\left(1-\frac{T_e\bullet T_X}{T_{g,1}\bullet T_{g,2}}\right)+COP_{AC}\right]}} \tag{34}$$

the $PXR_3 > PXR_1$, if

$$T_{c,2}>\left[\frac{\Delta T_c^{\,2}}{4}+\frac{T_e\bullet T_X\bullet COP_{AC}}{\left(1-\frac{\eta_{sys,AH}}{100}\right)\bullet\left(1-\frac{T_{K,2}\bullet T_X}{T_{g,1}\bullet T_{g,2}}\right)+COP_{AC}}\right]^{0,5}-0,5\bullet\Delta T_c,[K] \tag{35}$$

and the $PXR_3 > PXR_2$, if

$$T_{c,2}>\left[\frac{\Delta T_c^{\,2}}{4}+\frac{T_e\bullet T_X\bullet COP_{RC}}{COP_{RC}+1-\frac{\eta_{sys,RH}}{100}}\right]^{0,5}-0,5\bullet\Delta T_c,[K] \tag{36}$$

The condenser of the machine with a mechanical compressor heats the external air. Thus, the next selected temperature is the external air temperature, and $\Delta T_h = T_{h,2}$-$T_{h,1}$. The equation (31) does not include "$T_{h,1}$", so only two equations can be given. The $PXR_1 > PR_2$, if:

$$T_{h,1,R}> -0,5\bullet\Delta T_h+\sqrt{\frac{\Delta T_h^{\,2}}{4}+\frac{T_{K,2}\bullet T_X\bullet(COP_{RC}+1)}{COP_{RC}+\left[1-\frac{T_{K,2}\bullet T_X}{T_{g,1}\bullet T_{g,2}}\right]\bullet\frac{\alpha_{term}\bullet\eta_{term}}{\alpha_{elect}\bullet\eta_{elect}}\bullet\left(1-\frac{\eta_{sys,AC}}{100}-\frac{\eta_{sys,AH}}{100}\right)+\frac{\eta_{sys,RC}}{100}}} \tag{37}$$

and the $PXR_3 > PXR_2$, if:

$$T_{h,1}>\left[\frac{\Delta T_h^{\,2}}{4}+\frac{T_{K,2}\bullet T_X\bullet COP_{HC}}{COP_{RC}+\frac{\eta_{sys,Rc}}{100}}\right]^{0,5}-0,5\bullet\Delta T_h,[K] \tag{38}$$

Case study

The examined machines

The energy production system at the Clinical Centre of the University of Debrecen was built over time in stages. The energy production system contains (of course, among other machines) an absorption chiller (York YIA-HW-6C4-50), a chiller with a mechanical compressor (York YAES-0625-SB), and two identical gas engines (Caterpillar 3412, 1500 rpm). Even in the summer, the Clinical Centre requires a continuous supply of electrical power, cooling capacity, and heating energy flow. The integration of the Centre's energetic subsystems is constantly ongoing. In the following, it is examined from energetic and exergetic points of view if the system shown in Fig. 1 is implemented with the Centre's machines.

The main data's of the machines are summarised in Table 4 at the design condition:

Gas engines are operated continuously at full capacity.

It is advisable to examine the machines more carefully before potential interconnection. First, how values of "COP_R" and "η_{sys}" in the cooling mode of the two chillers change for the design condition is investigated when both evaporating and condensing temperatures can be varied by up to ± 5 °C.

According to Fig. 3, compared to the chiller with a mechanical compressor, the two indicators of the absorption chiller are higher sensitivity to the changes in the two temperatures.

How much of the exergy content of produced cooling capacity, from the exergy content of 1 MW of the energy flow operating the chillers, is examined (Fig. 4). All while changing the evaporation and condensation temperatures by a maximum of ± 5 °C. The chilled water temperature

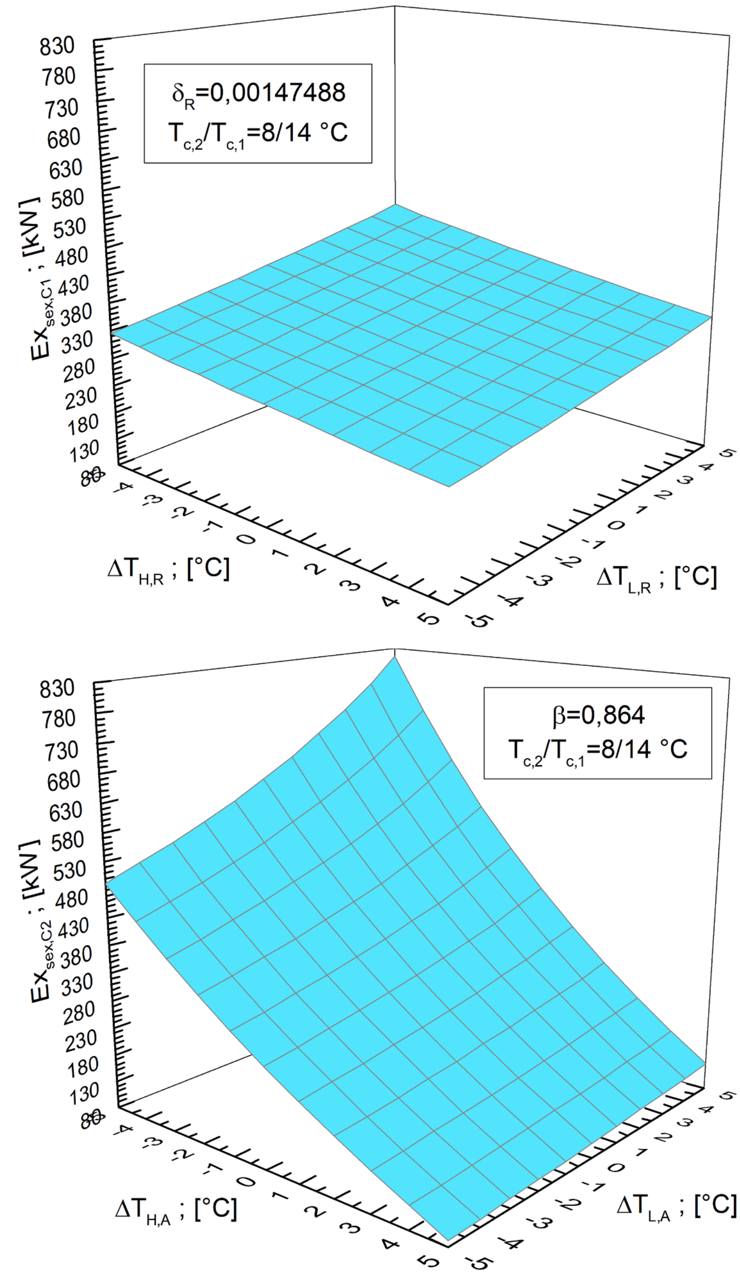

Fig. 4. Variation of the exergy content of the produced cooling capacity due to changes in the evaporating and condensing temperatures for **a)** the chiller with a mechanical compressor; **b)** the absorption chiller.

was 8/14 °C for both machines.

Based on Fig. 4, the exergy content of the produced cooling capacity is almost the same at the evaporation and condensation temperatures of the initial state (326.43 and 313.52 kW) while varying these temperatures by no more than 5–5 °C, a significant difference can be obtained (e. g. if T_L-5 °C and T_H + 5 °C: 416.94 and 814.88 kW).

Interconnection of the examined machines

If the four examined machines are connected, as shown in Fig. 1, they can produce three forms of energy concurrently. Thus, the calculations may account for the possibility that the heat flow and electrical power produced by gas engines do not have to be fully exploited by the heat pumps but can be utilized by building systems, for example. By using the results, the system can be examined not only quantitatively but also qualitatively. By the three operating modes, it can be taken into account that not all machines in a complex system are necessarily in operation (e. g., due to cost savings or maintenance problems).

However, if a system can produce multiple energy types, one type can be highlighted and optimized for that. Because the current case study treats the three energy types equally and does not account for seasonal changes in demand, it cannot optimize the system for only one energy type.

The consumption shares ("α_{term}" and "α_{elect}") must be established for

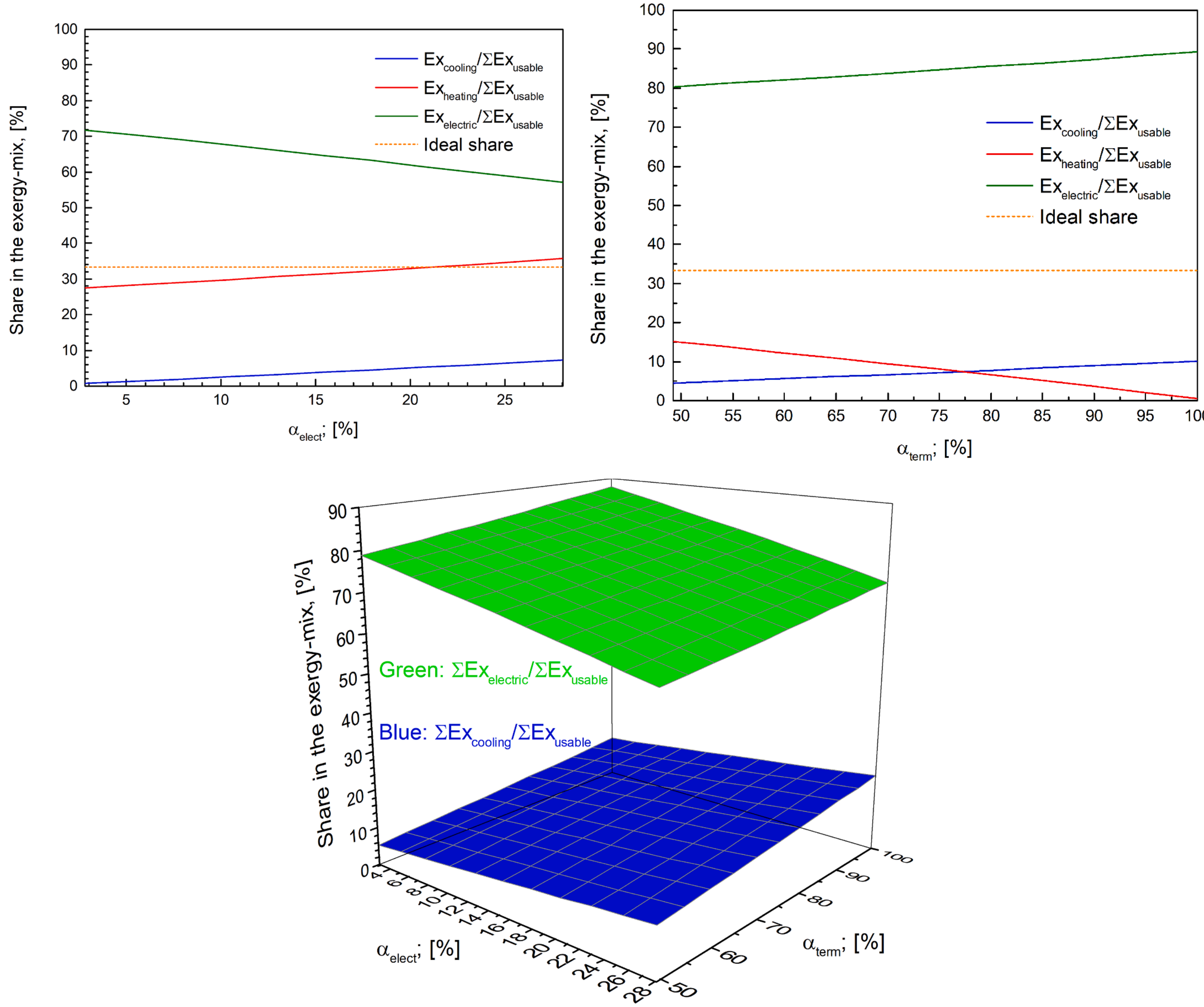

Fig. 5. The ratio between the exergy content of each type of produced energy and the exergy content of the total generated energy **a)** the 1.operating mode **b)** the 2. operating mode **c)** the 3. operating mode: cooling capacity and electrical power; **d)** the 3. operating mode: heat energy flow.

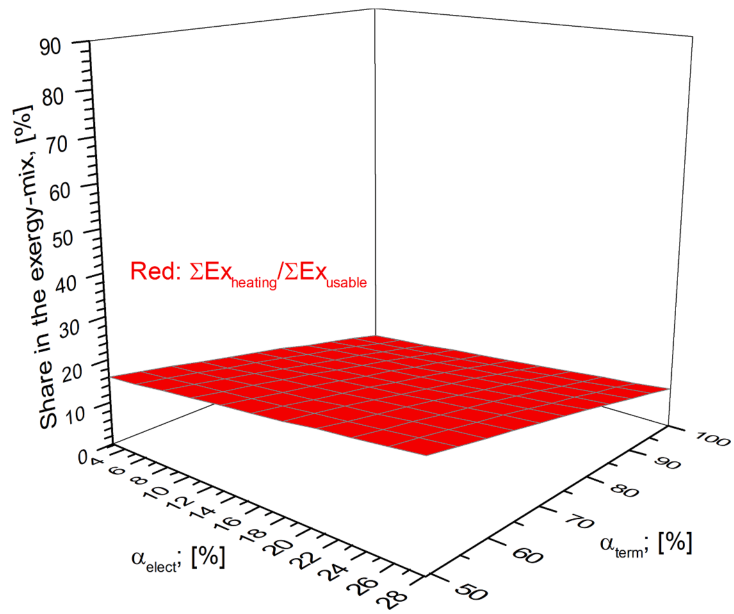

Fig. 5. (*continued*).

alignment. These latter values can theoretically vary between 0.0 and 1.0, but if the cooling capacity control of the two machines is taken into account and the gas engines are still running at full load, the value of "α_{elect}" and "α_{term}" can be changed between 2.81 and 28.05 % and 49.20–100 %, respectively. In the following, there is the ideal case to be where the exergy content of the energy forms generated is the same (i.e., their share in the exergy mix is 33.33 %).

Fig. 5 shows how the exergy content of each energy type in the common exergy-mix changes as a function of values of "α_{elect}" and "α_{term}". The 1. operating mode is shown in Fig. 5a, the 2. operating mode is shown in Fig. 5b, and the 3. operating mode is shown in Fig. 5c and 5d.

Based on Fig. 5, it is impossible to determine such consumption shares in this case that the exergy content of all energy types is the same. In closest-to-ideal case, the operational values of the examined system are provided in Table 5.

In the following, the consumption shares in the table will be considered. It is examined which operating mode is the best choice from an energetic and exergetic point of view. Based on equations (27)–(29), it is always preferable to use the 3. operating mode from an energy point of view. However, which is the second-best choice depends on several things. The critical generator temperature as a function of the two parameters influenced by the quantitative control („β" and „δ_R") is shown in Fig. 6.

As shown in Fig. 6, the critical generator temperature depends nearly linearly on "β" and "δ_R". A higher generator temperature is required for the increasing "β" (based on Fig. 6a), while the critical generator temperature is reduced by increasing "δ_R" (according to Fig. 6b). The more efficient heat pumps require a higher critical generator temperature due to the maximum value of the "COP" in cooling mode belonging to "β_{max}" and "$\delta_R = 0$", respectively.

From an exergetic point of view, the response is not already evident. The choice was examined as a function of the supply temperature of chilled water (Fig. 7a) and the external air temperature (Fig. 7b), as well.

According to Fig. 7, there will never be a case where the highest value of the primary exergetic ratio can be achieved with the 3. operating mode. Based on Fig. 7a, from an exergetic point of view, below $T_{c,2}$ = 15.67 °C, only the machine with a mechanical compressor should cooperate with the gas engine and only the absorption machine above this temperature. Therefore, if chilled water at a higher temperature is required by the cooling system, it can be more advantageous to use the 2. operating mode instead of 1. mode. Fig. 7b shows that if the external air is less than $T_{h,1}$ = 32.22 °C, then a better choice is to use the 2. operating mode, while above this temperature (until the value of "$T_{h,1}$" approaches the value of "$T_{H,R}$"), using the 1. operating mode is preferable.

Discussion

The results and the case study show that the different operating modes can achieve various "PER" values. For the closest-to-ideal case, the highest "PER" value can be achieved by 3. operating mode (1.73), followed by 1. operating mode (1.39), and 2. operating mode (1.18). Similar values can also be observed in the relevant research, e.g., Sun & Guo [19] achieved 1.81 or Liu et al. [21] 1.5 "PER" value, whereas Zhang et al. [24] could achieve in summer 1.167 "PER" value for an office building. For a trigeneration GEACHP system, one of the highest "PER" values (1.84) was observed by Sun [22].

The question may arise: Can this value be reached or exceeded with the analysed system configuration by replacing the existing machines with new, higher-efficiency devices? Of the three machine types, the two heat pumps have a higher potential to increase efficiency than the gas engine. Fig. 8 shows the "PER" values of the examined system by new heat pumps with a higher "COP_C" operating at the same temperature conditions.

Based on Fig. 8, PER = 1.91 (Fig. 8a) in 1. operating mode, 1.46 (Fig. 8c) in 2. operating mode, and 2.52 (Fig. 8e) in 3. operating mode can be achieved. Meanwhile, the change in "PXR" values (Fig. 8b, 8d, 8f) can be up to one order of magnitude lower than the change in "PER" values.

Table 5
The result of the alignment for the closest-to-ideal.

			Operation mode 1.	Operation mode 2.	Operation mode 3.
Consumption share	Electrical	α_{elect}; [%]	28.04	0	28.04
	Thermal	α_{term}; [%]	0	49.20	49.20
Generated cooling capacity	Quantity	ΣQ_0; [kW]	594.6	364.2	958.8
	Exergy content	ΣEx_0; [kW]	71.1	43.6	114.7
Generated heat flow	Quantity	ΣQ_H; [kW]	1880.7	1432.4	2244.9
	Exergy content	ΣEx_H; [kW]	349.5	145.9	212.9
Generated electrical power	Quantity	ΣP_{elect}; [kW]	558.8	776.7	558.8
	Exergy content	ΣEx_{elect}; [kW]	558.8	776.7	558.8
Primary energy ratio		PER; [-]	1.39	1.18	1.73
Primary exergy ratio		PXR; [-]	0.43	0.43	0.39

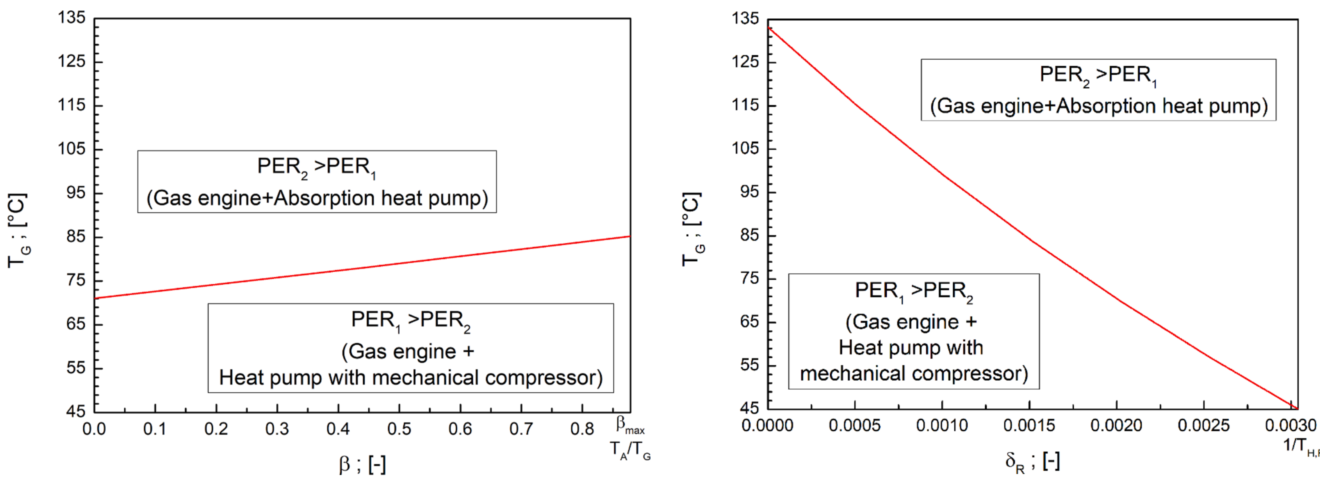

Fig. 6. The critical generator temperature depends on **a)** „β" **b)** „δ_R".

Conclusion

Several concepts and even more operating modes are possible for the GECAHP systems. This article examined a GECAHP system concept that implements trigeneration and can operate in three different operating modes. It had to be taken into account (by applying the consumption shares) that the energies produced by the gas engine do not have to be fully utilized by the heat pumps to accomplish trigeneration. And the three operating modes allow the operators to avoid running both heat pumps, e.g., in the case of reduced demand or maintenance problems. The three examined operating modes were also compared from an energetic and exergetic point of view. For the comparison, the primary exergy ratio ("PXR"), which is analogous to the primary energy ratio ("PER"), had to be introduced. Thus, similar to quantitative analysis, qualitative analysis can also be performed.

During the energetic and exergetic comparison, based on the "COP" and "η_{sys}" values, respectively, were used to decide which operating mode was the better option. Simplified equations to determine the values of "PER" and "PXR" were developed to facilitate comparison. For this, it was necessary using to the "COP_{RC}" and "COP_{AC}" values by the main operating temperatures and a factor describing the quantitative control of the machine. It is available in previous research for the

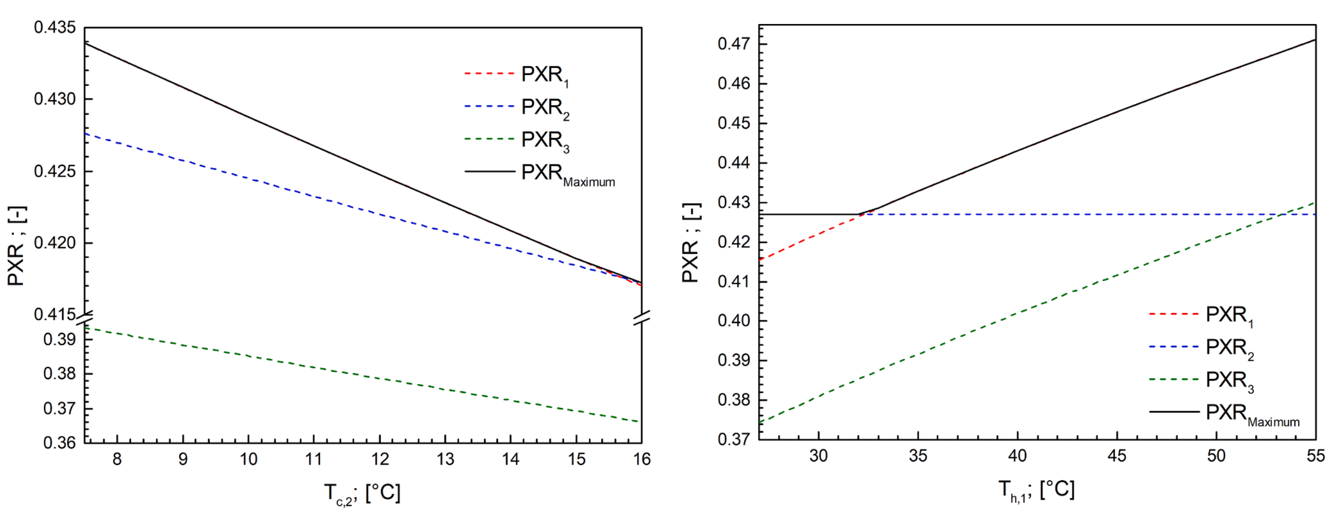

Fig. 7. The value of primary exergy ratio depends on the variation of the **a)** "$T_{C,2}$" **b)** "$T_{h,1}$".

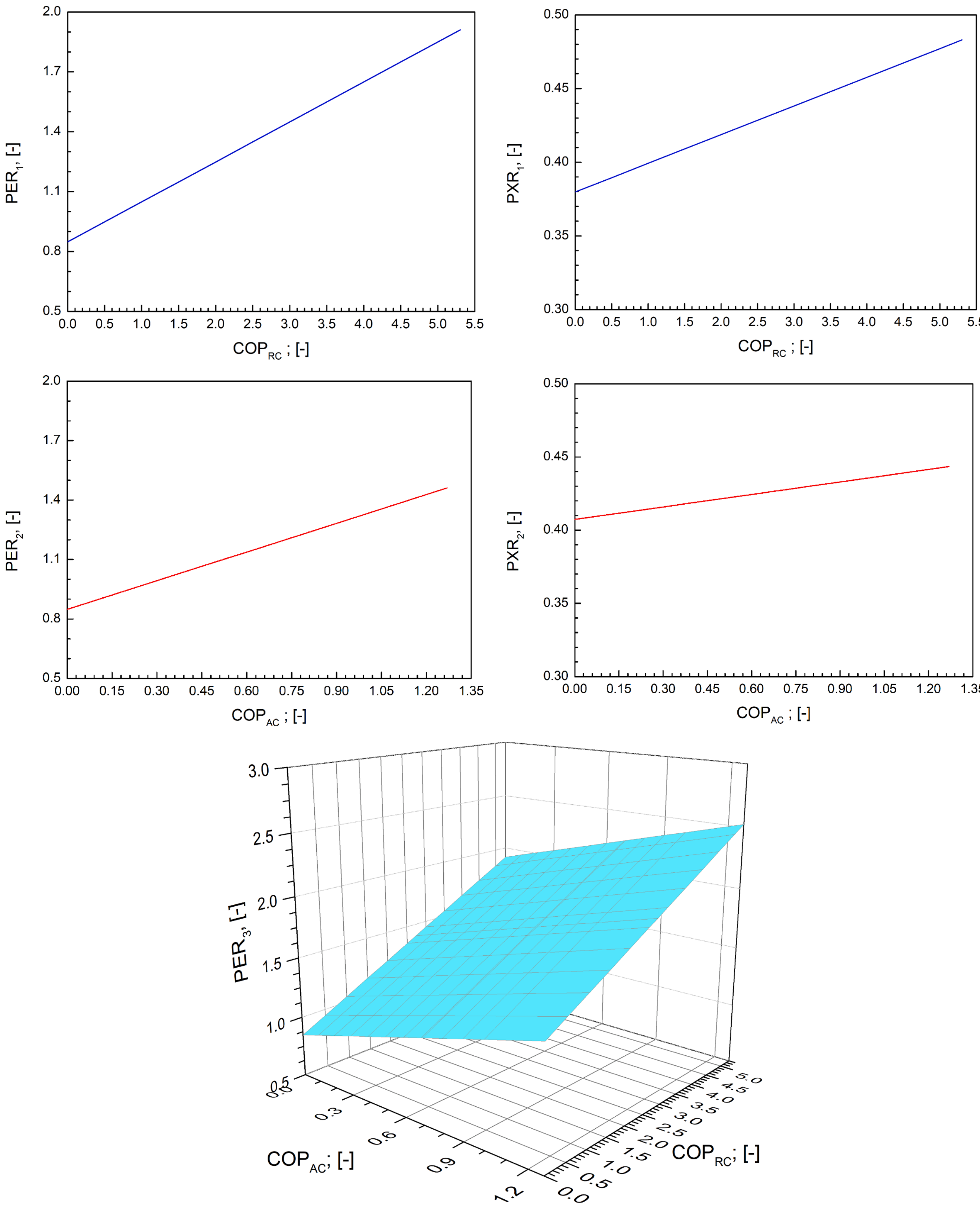

Fig. 8. The PER and PXR values of the system with new heat pumps **a)** 1. operating mode, PER; **b)** 1. operating mode, PXR; **c)** 2. operating mode, PER; **d)** 2. operating mode, PXR; **e)** 3. operating mode, PER; **f)** 3. operating mode, PXR.

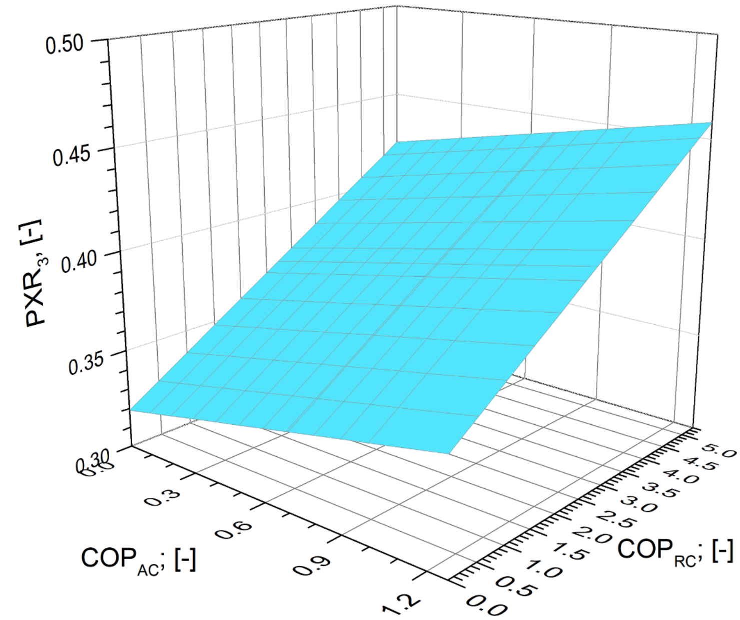

Fig. 8. (*continued*).

absorption machines, while it had to be defined by a new coefficient ("δ_R") in this article for the heat pump with a mechanical compressor.

Generally, it is practical if the equations containing parameters that are not directly or are difficult to measure are also given in other forms. Therefore, the results of comparisons are also presented at a few selected temperatures, as measuring the values of "COP" and "η_{sys}" can be challenging. Furthermore, it is also practical to examine these equations through a case study to more understandable and their possible hidden mistakes. Therefore, a potential interconnection of the machines of the Clinical Centre of the University of Debrecen is analysed at the design condition. Based on this case study, several conclusions can be made. From an energy point of view, the best option is the 3. operating mode (operating all three machines) in all cases, but the second-best option can change. The 2. operating mode (using the gas engine and absorption chiller) is the second-best option if the generator temperature is above 85.02 °C, and if it is below 85.02 °C, the 1. operating mode (working the gas engine and chiller with a mechanical compressor) is the second-best choice. From an exergetic point of view, the worst option is the 3. operating mode, but the best option varies. For example, if the cooling system requires chilled water at a higher temperature ($T_{c,2}$ greater than 15.67 °C), it is more advantageous to choose the 2. operating mode from an exergetic point of view. Or, if the external air temperature is below 32.22 °C, it is still preferable to use the 2. operating mode from an exergetic point of view.

Funding

Project no. TKP2021-NKTA-34 has been implemented with the support provided from the National Research, Development and Innovation Fund of Hungary, financed under the TKP2021-NKTA funding scheme.

CRediT authorship contribution statement

Gábor L. Szabó: Conceptualization, Methodology, Investigation, Data curation, Writing – original draft, Writing – review & editing, Visualization, Supervision.

Declaration of Competing Interest

The authors declare that they have no known competing financial interests or personal relationships that could have appeared to influence the work reported in this paper.

Data availability

Data will be made available on request.

References

[1] M. Santamouris, Cooling the buildings – past, present and future, Energy Build. 128 (2016) 617–638, https://doi.org/10.1016/j.enbuild.2016.07.034.

[2] X. Li, W. Wu, C.W.F. Yu, Energy demand for hot water supply for indoor environments: Problems and perspectives, Indoor Built Environ. 24 (1) (2015) 5–10, https://doi.org/10.1177/1420326X14564285.

[3] F. Kalmár, T. Kalmár, Interrelation between mean radiant temperature and room geometry, Energy Build. 55 (2012) 414–421, https://doi.org/10.1016/j.enbuild.2012.08.025.

[4] I. Csáky, Analysis of daily energy demand for cooling in buildings with different comfort categories—Case study, Energies 14 (15) (2021) pp, https://doi.org/10.3390/en14154694.

[5] F. Szodrai, Á. Lakatos, Különböző éghajlati viszonyoknak kitett épületek fűtési energiafelhasználásának csökkentése hőszigeteléssel, Energiagazdálkodás 57 (3–4) (2016) 26–29.

[6] Z. Verbai, I. Csáky, F. Kalmár, Balance point temperature for heating as a function of glazing orientation and room time constant, Energy Build. 135 (2017) 1–9, https://doi.org/10.1016/j.enbuild.2016.11.024.

[7] I. Csáky, F. Kalmár, Effects of thermal mass, ventilation, and glazing orientation on indoor air temperature in buildings, J. Build. Phys. 39 (2) (2015) 189–204, https://doi.org/10.1177/1744259115579060.

[8] N. Mirl, F. Schmid, K. Spindler, Reduction of the return temperature in district heating systems with an ammonia-water absorption heat pump, Case Studies in Thermal Engineering 12 (May) (2018) 817–822, https://doi.org/10.1016/j.csite.2018.10.010.

[9] Á. Lakatos, F. Kalmár, I. Csáky, Material selection in order to minimize the heat loss of piping based on measurements and calculations, AIP Conf. Proc. 2186 (December) (2019), https://doi.org/10.1063/1.5137984.

[10] M. Sheykhi, M. Chahartaghi, M.M. Balakheli, B.A. Kharkeshi, S.M. Miri, Energy, exergy, environmental, and economic modeling of combined cooling, heating and power system with Stirling engine and absorption chiller, Energy Convers. Manage. 180 (2019) 183–195.

[11] D. Xu, M. Qu, Energy, environmental, and economic evaluation of a CCHP system for a data center based on operational data, Energy Build. 67 (2013) 176–186, https://doi.org/10.1016/j.enbuild.2013.08.021.

[12] P.J. Mago, L.M. Chamra, Analysis and optimization of CCHP systems based on energy, economical, and environmental considerations, Energy Build. 41 (10) (2009) 1099–1106, https://doi.org/10.1016/j.enbuild.2009.05.014.
[13] M.M. Balakheli, M. Chahartaghi, M. Sheykhi, S.M. Hashemian, N. Rafiee, Analysis of different arrangements of combined cooling, heating and power systems with internal combustion engine from energy, economic and environmental viewpoints, Energy Convers. Manage. 203 (October) (2019) 2020, https://doi.org/10.1016/j.enconman.2019.112253.
[14] J. Wang, J. Wu, H. Wang, Experimental investigation of a dual-source powered absorption chiller based on gas engine waste heat and solar thermal energy, Energy 88 (2015) 680–689, https://doi.org/10.1016/j.energy.2015.05.103.
[15] D.W. Wu, R.Z. Wang, Combined cooling, heating and power: A review, Prog. Energy Combust. Sci. 32 (5–6) (2006) 459–495, https://doi.org/10.1016/j.pecs.2006.02.001.
[16] W. Ma, J. Fan, S. Fang, N.M.S. Hassan, Y. Zhang, X. Wu, Y.i. Li, R. Hu, G. Liu, Energy efficiency indicators for combined cooling, heating and power systems, Energy Convers. Manage. 239 (2021) 114187.
[17] A. Hepbasli, Z. Erbay, F. Icier, N. Colak, E. Hancioglu, A review of gas engine driven heat pumps (GEHPs) for residential and industrial applications, Renew. Sustain. Energy Rev. 13 (1) (2009) 85–99, https://doi.org/10.1016/j.rser.2007.06.014.
[18] E. Elgendy, J. Schmidt, Optimum utilization of recovered heat of a gas engine heat pump used for water heating at low air temperature, Energy Build. 80 (2014) 375–383, https://doi.org/10.1016/j.enbuild.2014.05.054.
[19] Z.G. Sun, K.H. Guo, Cooling performance and energy saving of a compression-absorption refrigeration system driven by a gas engine, Int. J. Energy Res. 30 (13) (2006) 1109–1116, https://doi.org/10.1002/er.1205.
[20] F. Liu, F. Dong, A. Yan, Y. Li, C. Yan, J. Li, Heating performance of a parallel gas engine compression-absorption heat pump, Appl. Therm. Eng. 123 (2017) 1308–1317, https://doi.org/10.1016/j.applthermaleng.2017.05.049.
[21] F. Liu, F. Dong, Y. Li, L. Jia, Study on the heating performance and optimal intermediate temperature of a series gas engine compression-absorption heat pump system, Appl. Therm. Eng. 135 (2018) 34–40.
[22] Z.G. Sun, Experimental investigation of integrated refrigeration system (IRS) with gas engine, compression chiller and absorption chiller, Energy 33 (3) (2008) 431–436, https://doi.org/10.1016/j.energy.2007.10.017.
[23] H. Liu, Q. Zhou, H. Zhao, Experimental study on cooling performance and energy saving of gas engine-driven heat pump system with evaporative condenser, Energy Convers. Manage. 123 (2016) 200–208, https://doi.org/10.1016/j.enconman.2016.06.044.
[24] Q. Zhang, Z. Yang, N. Li, R. Feng, Y. Gao, The influence of building using function on the operating characteristics of the gas engine driven heat pump with energy storage system (ESGEHPs), Energy Build. 167 (2018) 136–151, https://doi.org/10.1016/j.enbuild.2018.02.039.
[25] T.J. Kotas, The Exergy Method of Thermal Plant Analysis, First ed., Butterworth-Heinemann, Essex, 1985.
[26] G.L. Szabó, F. Kalmár, Investigation of energy and exergy performances of radiant cooling systems in buildings – A design approach, Energy 185 (2019) 449–462, https://doi.org/10.1016/j.energy.2019.07.067.
[27] G.L. Szabó, Energy and exergy analysis of radiant cooling systems in buildings, University of Debrecen, 2020.
[28] G.L. Szabó, Exergetic optimization of absorption chillers – A case study, Case Stud. Therm. Eng. 28 (October) (2021), https://doi.org/10.1016/j.csite.2021.101634.
[29] H. Caliskan, A. Hepbasli, Energy and exergy analyses of ice rink buildings at varying reference temperatures, Energy Build. 42 (9) (2010) 1418–1425, https://doi.org/10.1016/j.enbuild.2010.03.011.
[30] R. Zhang, Z. Tian, F. Liu, C. Tian, Z. Ma, L. Jia, Research on waste heat recovery from gas engine for auxiliary heating: An emerging operation strategy to gas engine-driven heat pump, Int. J. Refrig 121 (2021) 206–215, https://doi.org/10.1016/j.ijrefrig.2020.09.015.
[31] R. Li, R. Ooka, M. Shukuya, Theoretical analysis on ground source heat pump and air source heat pump systems by the concepts of cool and warm exergy, Energy Build. 75 (2014) 447–455, https://doi.org/10.1016/j.enbuild.2014.02.019.
[32] F. Kalmár, G.L. Szabó, Analysis of thermal compressor efficiency in case of geothermal energy sources, Build. Serv. Eng. Res. Technol. 35 (3) (2014) 237–243, https://doi.org/10.1177/0143624413484601.